Original Article

circFADS2 inhibits ferroptosis associated with *IGF2BP2*-dependent *SLC7A11* m6A modification in colorectal cancer cells

Liangjun Jiang[1], Xianzhou Lu[2], Wei Li[2]

[1]Department of Gastroenterology, Affiliated Nanhua Hospital, University of South China, Hengyang, China; [2]Department of Hepatobiliary Surgery, Affiliated Nanhua Hospital, University of South China, Hengyang, China

Contributions: (I) Conception and design: L Jiang, X Lu; (II) Administrative support: L Jiang; (III) Provision of study materials or patients: W Li; (IV) Collection and assembly of data: X Lu; (V) Data analysis and interpretation: W Li; (VI) Manuscript writing: All authors; (VII) Final approval of manuscript: All authors.

Correspondence to: Xianzhou Lu, MM; Wei Li, MD. Department of Hepatobiliary Surgery, Affiliated Nanhua Hospital, University of South China, No. 336 Dongfeng South Road, Zhuhui District, Hengyang 421002, China. Email: Lxz0734@126.com; liweiping0734@126.com.

Background: Colorectal cancer (CRC) is one of the most common malignancies worldwide, and its pathogenesis is highly complex. The aim of this study was to explore the mechanism of action of *circFADS2*- and *IGF2BP2*-mediated *SLC7A11* m6A modification in CRC.

Methods: *In vitro* experiments were conducted to knock down *circFADS2* and overexpress *SLC7A11* in CRC cells, and *circFADS2* expression was detected by reverse transcription quantitative polymerase chain reaction (RT-qPCR); Cell Counting Kit-8 (CCK-8) and colony formation experiments were used to detect cell proliferation; cell migration was detected by Transwell; terminal deoxynucleotidyl transferase dUTP nick end labeling (TUNEL) was used for detection of cell apoptosis; western blot (WB) was employed for detection of *SLC7A11* expression; the levels of malondialdehyde (MDA), glutathione (GSH), reactive oxygen species (ROS), and Fe^{2+} levels were detected; and messenger RNA (mRNA) stability testing, nuclear cytoplasmic separation experiments, RNA immunoprecipitation, fluorescence in situ hybridization (FISH), and immunofluorescence (IF) were used to verify the binding and mechanism of action of *circFADS2*, *IGF2BP2*, and *SLC7A11* mRNA. *In vivo* experiments were conducted by injecting CRC cells from each group subcutaneously into the right side of mice, and the growth of tumor cells was measured in each group *in vivo*.

Results: After knocking down *circFADS2*, the expression of *circFADS2* was downregulated in CRC cells. There was a significant reduction in cell proliferation and migration and a significant increase in cell apoptosis. The expression of *SLC7A11* was significantly reduced; MDA content significantly decreased; GSH levels decreased; ROS levels increased; and the concentration of Fe^{2+} significantly increased. After *circFADS2* knockdown, the growth of CRC cells *in vivo* was inhibited. In addition, mRNA stability testing showed that *circFADS2* knockdown significantly reduced the stability of *SLC7A11* mRNA. The nuclear cytoplasmic separation experiment showed that *circFADS2* was mainly expressed in the cytoplasm. RNA immunoprecipitation indicated a binding relationship between *IGF2BP2* and *circFADS2*, as well as between *IGF2BP2* and *SLC7A11* mRNA. The results of FISH and IF analysis showed that *circFADS2*, *IGF2BP2*, and *SLC7A11* mRNA were co-localized with *IGF2BP2* in the cytoplasm.

Conclusions: *circFADS2* facilitates the formation of the *circFADS2/IGF2BP2/SLC7A11* mRNA-protein complex, thereby enhancing the m6A methylation of *SLC7A11*. This process significantly promotes ferroptosis in CRC cells.

Keywords: Colorectal cancer (CRC); ferroptosis; *circFADS2*; *IGF2BP2*; *SLC7A11*

Submitted Dec 27, 2024. Accepted for publication Mar 03, 2025. Published online Apr 27, 2025.
doi: 10.21037/jgo-2024-1014
View this article at: https://dx.doi.org/10.21037/jgo-2024-1014

Introduction

Colorectal cancer (CRC) is a common cancer, the its incidence rate and mortality of which among young people are rising (1). Although the therapeutic approaches for CRC have been improved, symptoms of CRC only appear in late stages, and many patients are diagnosed with late-stage CRC at their first visit, resulting in relatively low cure rates and 5-year survival rates for patients (2). Therefore, understanding the potential molecular mechanisms underlying CRC is of enormous importance for developing novel treatment methods.

Iron-induced cell death (ferroptosis) is a cell death pattern distinct from apoptosis, which occurs due to the accumulation of iron or the consumption of antioxidant glutathione (GSH), leading to an increase in lipid peroxidation during steady-state turnover (3). Ferroptosis can inhibit tumor progression under certain circumstances (4); N6 methyladenosine modification enhances the anti ferroptotic ability of hepatoblastoma by inhibiting the deacetylation of *SLC7A11* messenger RNA (mRNA), a member of the solute carrier family 7 (5). *SLC7A11* is crucial for the uptake of cysteine, synthesis of GSH, and inhibition of ferroptosis (6). *SLC7A11* is considered to play an important role in the ferroptosis process of tumor cells (7-9). Downregulation of *SLC7A11* can promote ferroptosis in tumor cells, thereby exerting tumor suppressive functions (10). Existing studies have suggested that inducing ferroptosis may have a synergistic effect in tumor treatment (11,12). Therefore, exploring the mechanism of *SLC7A11*-induced ferroptosis may provide new insights for the development of CRC treatment strategies.

Circular RNA (circRNA) is mainly produced through a special alternative splicing method and is a non-coding RNA molecule (13). Currently, circRNA is known to play a role in various physiological processes (14), and also regulates gene expression by binding to specific mRNA (15). *CircMAP2K4* upregulates *YTHDF1* through m6A RNA methylation, thereby promoting cancer progression (16). According to a previous study, increased expression of *circFADS2* is associated with lower overall survival rates in cancer patients (17). In addition, *circFADS2* is the most significantly upregulated circRNA in CRC tissue, and its upregulation is closely related to the size, depth of invasion, metastasis, and poor prognosis of CRC (18). Therefore, we speculate that *circFADS2* may play a role in CRC by regulating mRNA methylation modification.

M6A is considered one of the most abundant base modifications in eukaryotic mRNA, involved in biological processes such as mRNA modification and stability (19). According to reports, *IGF2BP2* is an m6A reader that enhances mRNA stability by recognizing m6A modification sites (20). *IGF2BP2* has been shown to promote cancer progression by enhancing the stability of *SLC7A11* mRNA (21). Promoting *SLC7A11* expression can enhance GPX4 activity to inhibit ferroptosis in CRC cells, thereby promoting CRC tumorigenesis (11). This suggests that regulating *IGF2BP2*-mediated *SLC7A11* m6A modification may become an effective pathway for CRC treatment.

We speculated that *circFADS2* may inhibit ferroptosis in CRC cells by regulating *IGF2BP2*-mediated *SLC7A11* m6A modification. At present, there is no research to support the regulatory effect of *circFADS2* on *SLC7A11*. We explored the mechanism of action by knocking down *circFADS2* and overexpressing *SLC7A11* in CRC cell lines HT29 and HCT116, which may provide support for the treatment of CRC. We present this article in accordance with the ARRIVE and MDAR reporting checklists (available at https://jgo.amegroups.com/article/view/10.21037/jgo-2024-1014/rc).

Highlight box

Key findings

- Our study demonstrates the molecular mechanism by which *circFADS2* inhibits ferroptosis in colorectal cancer (CRC) cells by regulating *IGF2BP2*-mediated *SLC7A11* m6A modification.

What is known and what is new?

- Studies have shown that inducing ferroptosis can have a good synergistic effect in tumor treatment.
- We explored the mechanism of action by knocking down *circFADS2* and overexpressing *SLC7A11* in CRC cell lines HT29 and HCT116, suggesting a possible therapeutic method for the clinical treatment of CRC.

What is the implication, and what should change now?

- Our findings offer fresh perspectives on the molecular process underlying CRC ferroptosis and lay a scientific foundation for developing new treatment strategies.

Methods

Cell culture and processing

We prepared a protocol before the study without registration. CRC cell lines HCT116 and HT29 were purchased from Cytion (Eppelheim, Germany). Cells were

Table 1 The primer sequences for RT-qPCR

Gene	Primer sequences (5'-3')
circFADS2	Forward: TTTGTGTGTGCGTGTTGTTGG
	Reverse: ATGGAGGAGGCTTGGACATC
SLC7A11	Forward: TCCTGCTTTGGCTCCATGAACG
	Reverse: AGAGGAGTGTGCTTGCGGACAT
U6	Forward: CTCGCTTCGGCAGCACAT
	Reverse: TTTGCGTGTCATCCTTGCG
GAPDH	Forward: GTCTCCTCTGACTTCAACAGCG
	Reverse: ACCACCCTGTTGCTGTAGCCAA

RT-qPCR, reverse transcription quantitative polymerase chain reaction.

cultivated in Dulbecco's modified Eagle medium (DMEM, 11965092, Gibco, Waltham, MA, USA) containing 10% fetal bovine serum (FBS, 26140079, Gibco) and 1% penicillin streptomycin (15140122, Gibco) at 37 ℃ and 5% CO_2. When the cells were cultured to a confluence of 60–80%, lentiviral particles (purchased from VectorBuilder, Chicago, IL, USA) containing knockdown gene expression vectors (sh-*circFADS2* 1 #, sh-*circFADS2* 2 #, and sh-*circFADS2* 3 #) and overexpression gene expression vectors (oe-NC, oe-*SLC7A11*) were added for 48 hours, and antibiotics were added for cell screening.

Reverse transcription quantitative PCR

Total RNA was extracted using the TRIzol reagent (15596026, Invitrogen™, Waltham, MA, USA). Next, the extracted RNA was then quantified using a HD-UV90 spectrophotometer (Shandong Hold Electronic Technology Co., Weifang, China) as directed in the manual. After that, 2 μg of RNA was subjected to reverse transcription with the Vazyme DLR102 SynScript® III One-Step RT Kit (DLR102, Vazyme Biotech Co., Ltd., Nanjing, China) and microRNA (miRNA) First Strand cDNA Synthesis Kit (B532451, Sangon Biotech Co., Ltd., Shanghai, China) to create complementary DNA (cDNA). Later, the quantitative polymerase chain reaction (qPCR) analysis was performed in compliance with the instructions of the TB Green® Premix Ex Taq™ II (RR820A, Takara Holdings Inc., Kyoto, Japan). Subsequently, using *GAPDH* as an internal reference, the relative expression level (22) was calculated using the $2^{-\Delta\Delta Ct}$ method. The primer sequences are shown in *Table 1*.

Cell Counting Kit-8

A Cell Counting Kit-8 detection kit (C0037, Beyotime, Shanghai, China) was used for testing. Cells were inoculated (3×10^3/well) onto a 96 well plate and incubated. After 0, 12, 24, and 48 hours, cell samples were cultured at 37 ℃ for 2 hours with 10 μL CCK-8 and 90 μL serum-free medium, containing 95% air and 5% carbon dioxide. The optical density (OD) value was measured at a wavelength of 450 nm using a microplate reader (BioTek Instruments Inc, Winooski, VT, USA) to evaluate cell proliferation.

Colony formation assay

The cell suspension was diluted and each group of cells was inoculated into a cell culture dish at a density of 1,000 cells per dish. The cells were cultivated in a 37 ℃ 5% CO_2 and saturated humidity incubator for 2 weeks. The supernatant was discarded and the cells were fixed with 4% paraformaldehyde (158127, Sigma Aldrich, St. Louis, MO, USA) for 15 minutes. Then, the fixative was removed, 10% diluted Giemsa staining solution (48900, Sigma Aldrich) was added for 10 minutes, the staining solution was washed away, and the cells were air dried. Clones with more than 10 cells were counted under a microscope to evaluate cell proliferation.

Transwell

The upper chamber of the Transwell was seeded with 200 μL of serum-free DMEM containing 1×10^5 cells (A1896702, Thermo Fisher Scientific, Waltham, MA, USA), while the lower chamber contained 500 μL of DMEM medium supplemented with 10% FBS. After co-culturing for 48 hours, the upper chamber cells were removed, the lower chamber cells were fixed with 4% paraformaldehyde, stained with crystal violet solution (198099, Merck, Darmstadt, Germany), and finally observed and photographed under a Nikon Eclipse E200 microscope (Nikon Corp., Tokyo, Japan). Quantitative analysis of migrating cells was performed using ImageJ software (National Institutes of Health, Bethesda, MD, USA).

Reactive oxygen species

Cells were digested with trypsin, the cell pellet was resuspended in 1 mL of pre-diluted 2',7'-dichlorodihydrofluorescein diacetate (DCFH-DA) probe (C400, Thermo Fisher Scientific) solution (working concentration of 10 μM), and

left to sit at 37 ℃ in the dark for 30 minutes, with vortexing performed every 5 minutes, followed by centrifugation at 1,000 g and 25 ℃ for 5 minutes. Fluorescence images were obtained using a fluorescence microscope (Olympus, Tokyo, Japan) and analyzed using ImageJ software.

Terminal deoxynucleotidyl transferase dUTP nick end labeling

Trypsin was used to digest cells. The cells were fixed in a 4% formaldehyde solution for 20 minutes, then 0.1% Triton X-100 was added and incubated at room temperature for 5 minutes to allow permeabilization. The reaction solution was prepared by combining terminal deoxynucleotidyl transferase (TdT) with Alexa Fluor™ 488-dUTP: prepare the reaction solution according to the instructions of the terminal deoxynucleotidyl transferase dUTP nick end labeling (TUNEL) kit (C10617, Thermo Fisher Scientific). The reaction solution was added dropwise onto the sample and incubated at 37 ℃ for 1 hour. 4',6-diamidino-2-phenylindole (DAPI) staining solution (62248, Thermo Fisher Scientific) was then added dropwise onto the sample and incubated at room temperature in the dark for 20 minutes. Apoptotic cells were observed under a fluorescence microscope, and the apoptosis rate was determined by counting the total number of cells and the number of apoptotic cells (apoptosis rate = TUNEL positive cells/total cells * 100%).

Western blot (WB)

Radioimmunoprecipitation assay (RIPA) solution (89900, Thermo Fisher Scientific) was added to the cells which were then lysed on ice for 30 minutes and shaken every 5 minutes during this period. They were then centrifuged at 12,000 rpm for 10 minutes at 4 ℃ and the supernatant was collected. The protein concentration of each sample was measured using a bicinchoninic acid (BCA) protein detection kit (23227, Thermo Fisher Scientific). After separation with sodium dodecyl sulfate polyacrylamide gel electrophoresis (SDS-PAGE), the protein was transferred to a polyvinylidene fluoride (PVDF) membrane (88518, Thermo Fisher Scientific). After electroporation, the membrane was sealed with 5% skimmed milk powder for 1 hour. Following blocking, *SLC7A11* (1:1,000, PA1-16893, Thermo Fisher Scientific) and *GAPDH* (1:5,000, MA5-35235, Invitrogen) antibodies were added to treat the membrane, and incubated overnight at 4 ℃. Then, goat anti rabbit IgG HRP antibody diluted in 5% skim milk (1:10,000, 31460, Thermo Fisher Scientific) was added, followed by incubation at room temperature for 1 hour. Finally, the protein bands were developed using enhanced chemiluminescence (ECL) reagent (32106, Thermo Fisher Scientific) and analyzed for OD using ImageJ image analysis software with *GAPDH* as the internal reference.

Biochemical analysis

A reduced GSH Colorimetric Assay Kit (EIAGSHC, Thermo Fisher Scientific), MDA Kit (HY-K0319, MedChemExpress, Monmouth Junction, NJ, USA) and cell total iron colorimetric assay kit (EEA009, Thermo Fisher Scientific) was used to detect GSH, MDA, ROS, and Fe^{2+} in cells.

Animal modeling and processing

This study was approved by the Animal Committee of Affiliated Nanhua Hospital, University of South China (No. 20240302) and conducted in compliance with the national guidelines for the care and use of animals. The supplier of the 6-week-old male BALB/c nude mice (16–18 g) was Fujian Anbuli Biotechnology Co., Ltd. (Fujian, China). All animals were kept in a pathogen-free environment and were free to eat and drink in a 12-hour light/dark cycle, with room temperature of 21±2 ℃ and humidity ranging from 45% to 65%. Only healthy, 6-week-old male BALB/c nude mice without prior medical history were selected for the experiment. Twenty-four BALB/c nude mice were randomly divided into 4 groups (n=6): sh-NC, sh-*circFADS2*, sh-*circFADS2* + oe-NC, and sh-*circFADS2* + oe-*SLC7A11*. A subcutaneous injection of 1×10^6 stably transfected HT29 cells [suspended in 0.2 mL phosphate-buffered saline (PBS)] was administered into the right abdomen of BALB/c nude mice. After 7 days of vaccination, the long and short axes of the tumor were measured every 4 days, and the tumor volume (V) was calculated using the formula ($V=1/2 \times$ long axis $\times$ short axis^2). After the experiment was completed (day 28), the tumor volume was measured and the mice were euthanized via intraperitoneal injection of an excess (200 mg/kg) of pentobarbital sodium (57-33-0, Merck, Darmstadt, Germany). The tumor tissue was removed and weighed.

RNA immunoprecipitation

After the cells had been cultivated to a confluence degree

of 70–80%, the culture medium was removed and RIPA buffer containing protease and RNAse inhibitors was added for lysis for 30 minutes. Following centrifugation at 12,000 rpm for 15 minutes, the supernatant was collected. Incubation was performed with protein A/G magnetic beads with lysis buffer for 30 minutes, followed by washing with PBS. Then, *IGF2BP2* antibody (712137, Thermo Fisher Scientific) and IgG antibody (SAB5600195, Sigma Aldrich) were added and incubated overnight at 4 ℃, after which protein A/G beads (88802, Thermo Fisher Scientific) were added. The mixture was rotated and incubated for 2 hours to allow the antibody antigen complex to bind to the beads. The beads were then washed 3 times and centrifuged each time to remove the supernatant. Subsequently, proteinase K (20 mg/mL) was added for cross-linking. The purified RNA was extracted and analyzed by RT-qPCR.

Nuclear cytoplasmic separation experiment

SurePrep™ Nuclear or Cytolytic RNA Purification Kit (BP2805-50, Thermo Fisher Scientific) was used to treat cells with cell lysis buffer according to the instructions in the kit. The cells were then incubated on ice for 5–10 minutes to lyse the cell membrane and release cytoplasmic contents. According to the instructions of the reagent kit, nuclear extraction buffer was used to treat nuclear pellet. Following centrifugation at 10,000 ×g at 4 ℃ for 20 minutes, the supernatant was collected and precipitated for RT-qPCR analysis.

mRNA stability testing

Cells that had undergone knockdown of *circFADS2* and *IGF2BP2*, as well as negative control cells, were treated with 1 μg/mL transcription inhibitor Actinomycin D (J60148. LB0, Thermo Fisher Scientific) to block the synthesis of new mRNA. In order to assess the stability of the expression of *SLC7A11* mRNA, cells were collected at various time points (0, 1, 2, and 4 h) and tested by RT-qPCR.

Fluorescence in situ hybridization (FISH) and immunofluorescence

A FISH kit purchased from Sigma Aldrich was used to measure the fluorescence signal of the probe, and fluorescence image acquisition was completed using a Zeiss LSM 980 microscope (ZEISS, Oberkochen, Germany). Cells were fixed with 4% formaldehyde and incubated at room temperature for 30 minutes. Cell permeabilization was performed with 0.5% Triton X-100 treatment. The cell samples were mixed with 50 nM fluorescein isothiocyanate (FITC)-labeled *circFADS2* and *SLC7A11* mRNA probes purchased from Sigma Aldrich, and incubated at 37 ℃ for 4 hours in a wet box.

Immunofluorescence detection: cells were fixed with 4% formaldehyde and incubated at room temperature for 30 minutes. Cell permeabilization was performed using 0.5% Triton X-100 treatment. The sample was washed with pre-cooled saline-sodium citrate (SSC) buffer and *IGF2BP2* antibody was added (1:100, PA5-115396, Thermo Fisher Scientific) for overnight incubation at 4 ℃. Goat anti rabbit IgG H&L (Alexa Fluor® 647) (1 μg/mL, ab150079, Abcam, Cambridge, MA, USA) was added and incubated at room temperature in the dark for 2 hours. Then, 1 μg/mL DAPI (62248, Thermo Fisher Scientific) and incubate for 10 minutes. After sealing with DAPI Aqueous, Fluoroshield (ab104139, Abcam), the cells were viewed under a fluorescent microscope. ImageJ image analysis software was used to analyze the fluorescence images.

Statistical analysis

GraphPad Prism 9 (GraphPad Software, San Diego, CA, USA) was used for statistical analysis. Comparisons between 2 groups were performed using the *t*-test. For data involving 3 or more groups, 1- or 2-way analysis of variance (ANOVA) was used, followed by Tukey's post hoc test. A P value <0.05 indicated a statistical difference, and at least 3 replications of each experiment were conducted.

Results

Knocking down circFADS2 inhibits malignant behavior of CRC cells

RT-qPCR analysis revealed that *circFADS2* was upregulated in CRC cells (HT29 and HCT116) (*Figure 1A*). Knockdown of *circFADS2* was performed on CRC cells, and *circFADS2* expression was detected by RT-qPCR. The outcomes demonstrated that the downregulation of *circFADS2* was most significant in sh-*circFADS2* 1 # (*Figure 1B*). Based on the experimental results, we selected the infection of sh-*circFADS2* 1 # for subsequent experiments. Knocking down *circFADS2* obviously led to downregulation of *circFADS2* expression (*Figure 1C*). CCK-8 detection showed that knocking down *circFADS2* significantly reduced CRC

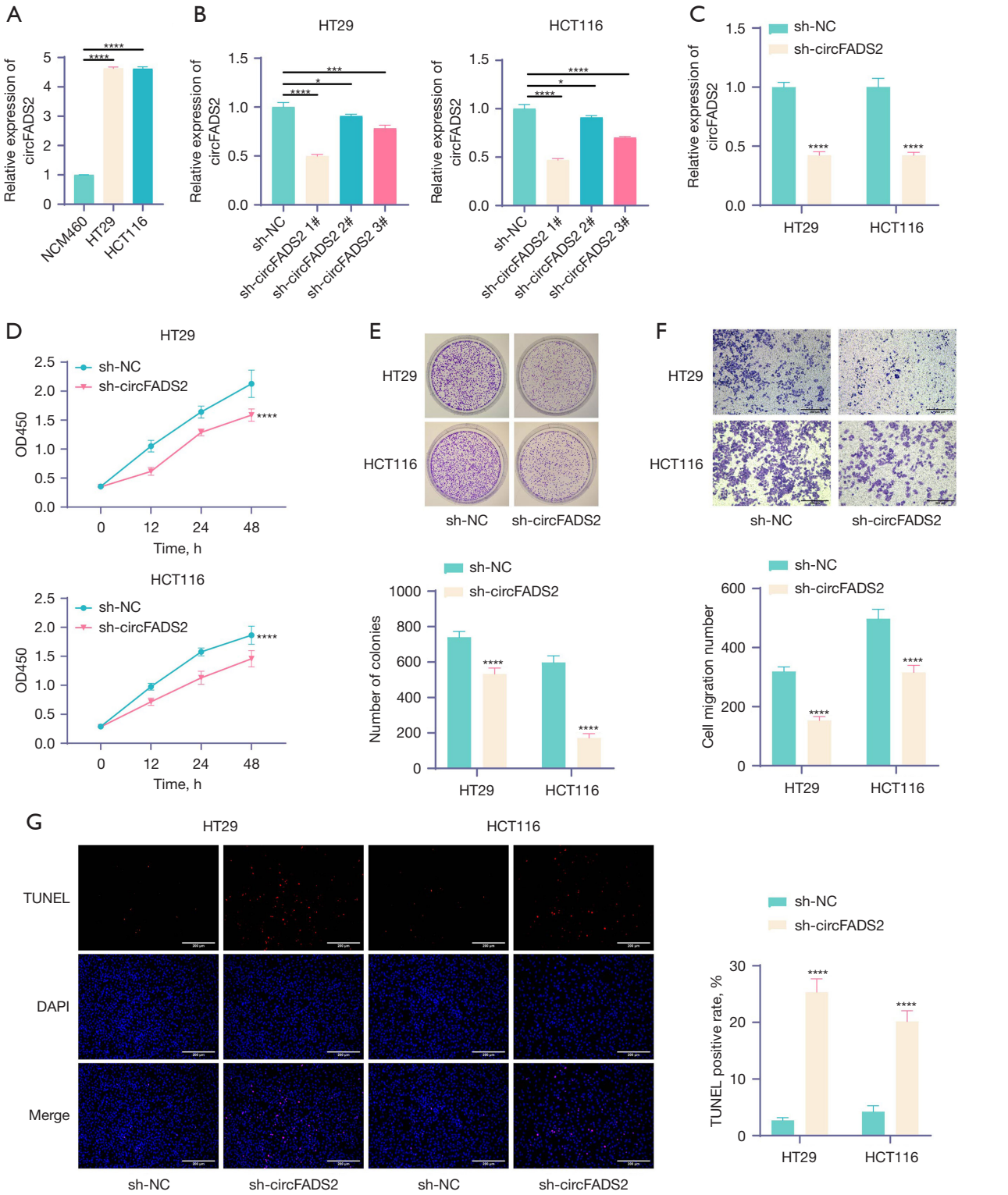

Figure 1 Knocking down *circFADS2* inhibits malignant behavior of CRC cells. (A-C) RT-qPCR was used to detect the expression of *circFADS2* in CRC cells. (D,E) CCK-8 and colony formation experiments were used to detect cell proliferation. (F) Transwell detection of cell migration. (G) TUNEL detection of cell apoptosis (n=3). Staining method: Giemsa staining (colony formation assay); crystal violet

staining (Transwell assay); Alexa Fluor™ 488-dUTP and DAPI staining (TUNEL assay). The magnification ratio of the image is 200 times (with a scale of 200 μm). *, P<0.05; ***, P<0.001; ****, P<0.0001. Three or more sets of data will be analyzed using one-way or two-way ANOVA, and Tukey's will be used for post hoc testing. ANOVA, analysis of variance; CRC, colorectal cancer; CCK-8, Cell Counting Kit-8; DAPI, 4',6-diamidino-2-phenylindole; RT-qPCR, reverse transcription quantitative polymerase chain reaction; TUNEL, terminal deoxynucleotidyl transferase dUTP nick end labeling.

cell proliferation (*Figure 1D*). The colony formation assay showed that downregulating the expression of *circFADS2* inhibited the ability of CRC cells to form clones (*Figure 1E*). The Transwell findings demonstrated that the migration ability of CRC cells decreased after the expression of *circFADS2* was reduced (*Figure 1F*). TUNEL detection showed that knockdown of *circFADS2* promoted apoptosis of CRC cells (*Figure 1G*). The outcomes demonstrated that knocking down *circFADS2* can inhibit the malignant behavior of CRC cells.

Knocking down circFADS2 promotes ferroptosis in CRC cells

WB detection showed that knocking down *circFADS2* significantly reduced the expression of ferroptosis-related protein *SLC7A11* in CRC cells (*Figure 2A*). In addition, after *circFADS2* knockdown, the GSH level in CRC cells significantly decreased, while the concentrations of MDA, ROS, and Fe^{2+} increased significantly (*Figure 2B-2E*). In BALB/c nude mice, CRC cells knocking down *circFADS2* were injected subcutaneously into the lower abdomen of the mice. In addition, knocking out *circFADS2* significantly reduced tumor growth and tumor weight in BALB/c mice (*Figure 2F*). The WB detection results showed that compared with the sh-NC group, the expression of ferroptosis related protein *SLC7A11* was reduced in the tumor tissues of BALB/c nude mice in the sh-*circFADS2* group (*Figure 2G*). The results indicate that knocking down *circFADS2* promotes ferroptosis in CRC cells.

The formation of stable complex circFADS2/IGF2BP2/SLC7A11 promotes the stability of SLC7A11 mRNA

The findings from nuclear cytoplasmic separation experiments indicated that *circFADS2* is mainly expressed in the cytoplasm (*Figure 3A*). RT-q-PCR detection showed that knocking down *circFADS2* significantly reduced the stability of *SLC7A11* mRNA. In addition, inhibiting *IGF2BP2* was also shown to reduce the stability of *SLC7A11* mRNA and decrease *SLC7A11* expression (*Figure 3B*). *IGF2BP2* is an m6A reader that enhances mRNA stability by recognizing m6A modification sites (20). The RNA immunoprecipitation (RIP) results indicated that there are interactions between *circFADS2* and *IGF2BP2*, as well as between *IGF2BP2* and *SLC7A11* mRNA (*Figure 3C*). The FISH and IF analysis results showed that *circFADS2* and *IGF2BP2* were co-localized in the cytoplasm of CRC cells, and *SLC7A11* mRNA was co-localized with *IGF2BP2* in the cytoplasm (*Figure 3D*). The results indicated that *circFADS2* promotes m6A methylation modification of *SLC7A11* mRNA by *IGF2BP2* through binding, thereby promoting *SLC7A11* expression.

circFADS2 promotes malignant behavior of CRC cells by regulating SLC7A11

Overexpression of *SLC7A11* was performed in *circFADS2* knockdown CRC cells (HT29 and HCT116). The results of RT-qPCR showed that compared with the sh-*circFADS2* + oe-NC group, *SLC7A11* was upregulated in the sh-*circFADS2* + oe-*SLC7A11* group (*Figure 4A*). CCK-8 detection showed that after upregulation of *SLC7A11*, CRC cell proliferation significantly increased (*Figure 4B*). The colony formation assay showed that further expression of *SLC7A11* increased CRC cell proliferation (*Figure 4C*). The Transwell results indicated that overexpression of *SLC7A11* promoted CRC cell migration (*Figure 4D*). TUNEL detection showed that overexpression of *SLC7A11* inhibited apoptosis in CRC cells (*Figure 4E*). The results showed that overexpression of *SLC7A11* reversed the inhibitory effect of knocking down *circFADS2* on the malignant behavior of CRC cells. This indicates that *circFADS2* promotes malignant behavior of CRC cells by regulating *SLC7A11*.

circFADS2 inhibits ferroptosis in CRC cells by regulating SLC7A11 expression

In the *in vitro* experiments, WB detection showed that overexpression of *SLC7A11* significantly increased

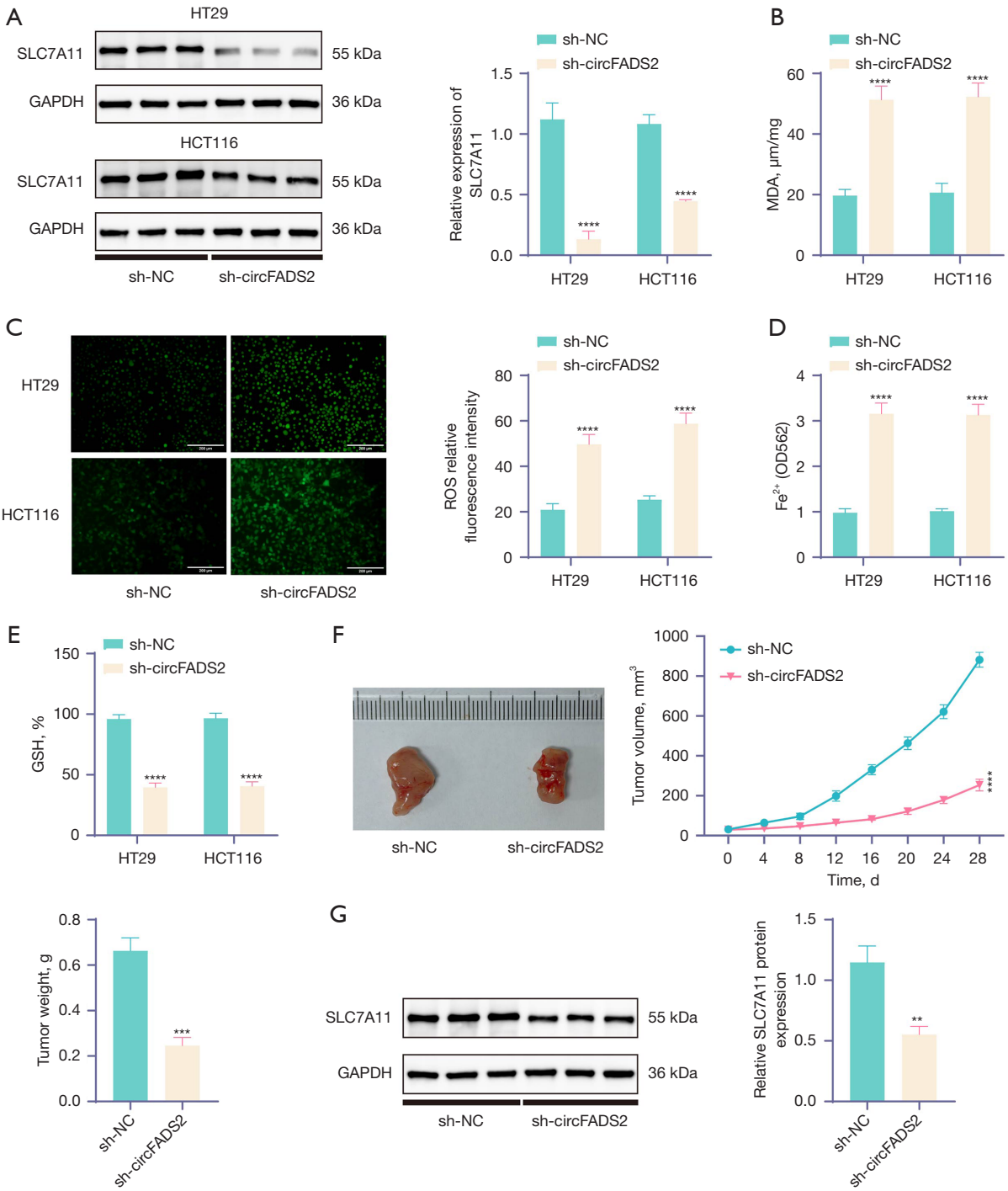

Figure 2 Knocking down *circFADS2* promotes ferroptosis in CRC cells. (A) WB detection of *SLC7A11* expression in CRC cells (n=3). (B-E) Detection of GSH, MDA, ROS, and Fe^{2+} levels in CRC cells (n=3). (F) Detection of the volume and weight of mouse tumors (n=6). (G) WB detection of *SLC7A11* expression in mice (n=6). Staining method: DCFH-DA staining (ROS assay). The magnification ratio of the image is 200 times (with a scale of 200 μm). **, P<0.01; ***, P<0.001; ****, P<0.0001. The detection between the two groups was analyzed using *t*-test. Two factor ANOVA will be used for three or more sets of data, and Tukey's will be used for post hoc testing. ANOVA, analysis of variance; CRC, colorectal cancer; DCFH-DA, 2',7'-dichlorodihydrofluorescein diacetate; GSH, glutathione; MDA, malondialdehyde; ROS, reactive oxygen species; WB, western blot.

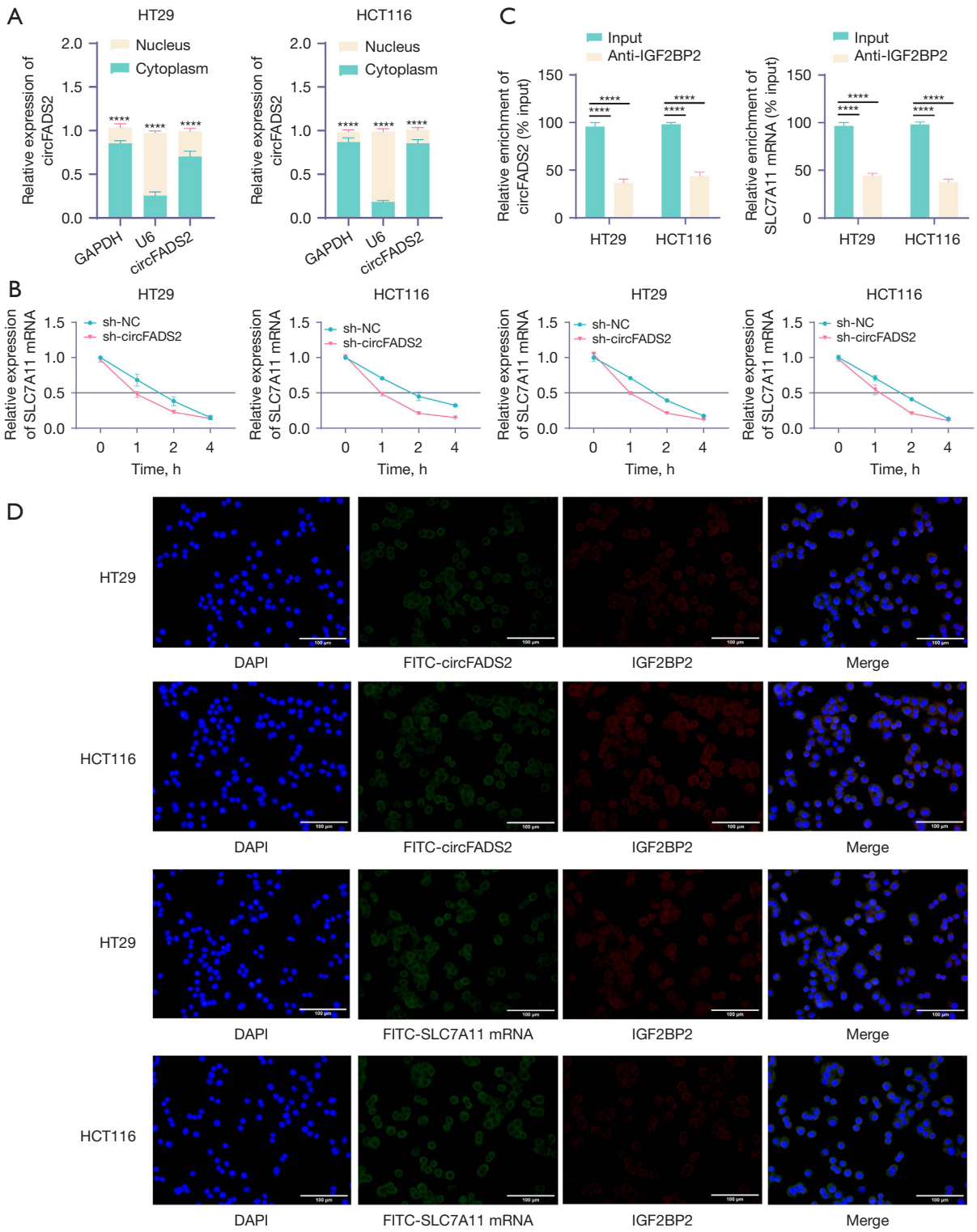

Figure 3 The formation of stable complex *circFADS2/IGF2BP2/SLC7A11* promotes the stability of *SLC7A11* mRNA. (A) Nuclear cytoplasmic separation experiment was used to detect *circFADS2* expression. (B) *SLC7A11* mRNA stability detection. (C) RNA immunoprecipitation detection of the binding relationship between *circFADS2* or *SLC7A11* mRNA and *IGF2BP2*. (D) FISH detection of co localization between *circFADS2*, *SLC7A11* mRNA, and *IGF2BP2* and *SLC7A11* mRNA. Staining method: FITC staining (FISH);

Alexa Fluor 647/DAPI staining (IF). The magnification ratio of the image is 400 times (with a scale of 100 μm). (n=3). ****, P<0.0001. Two factor ANOVA will be used for three or more sets of data, and Tukey's will be used for post hoc testing. ANOVA, analysis of variance; DAPI, 4',6-diamidino-2-phenylindole; FISH, fluorescence in situ hybridization; IF, immunofluorescence; FITC, fluorescein isothiocyanate; mRNA, messenger RNA.

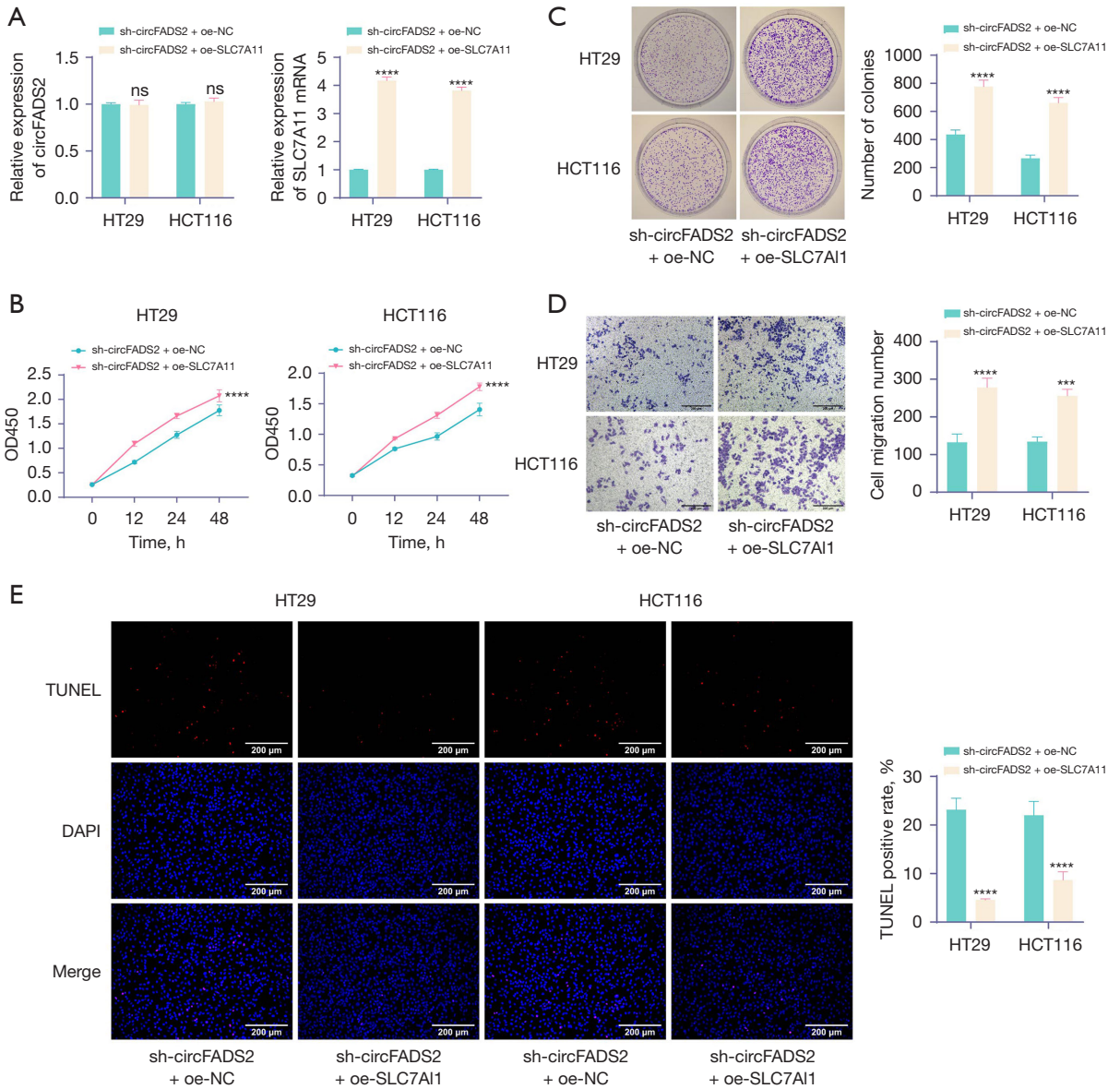

Figure 4 *circFADS2* promotes malignant behavior of CRC cells by regulating *SLC7A11*. (A) RT-qPCR was used to detect the expression of *circFADS2* and *SLC7A11*. (B,C) CCK-8 and colony formation detection for cell proliferation. (D) Transwell detection of cell migration. (E) TUNEL detection of cell apoptosis. Staining method: Giemsa staining (colony formation assay); crystal violet staining (Transwell assay); Alexa Fluor™ 488-dUTP and DAPI staining (TUNEL assay). The magnification ratio of the image is 200 times (with a scale of 200 μm). (n=3). ns, P>0.05; ***, P<0.001; ****, P<0.0001. Two factor ANOVA will be used for three or more sets of data, and Tukey's will be used for post hoc testing. ANOVA, analysis of variance; CRC, colorectal cancer; CCK-8, Cell Counting Kit-8; DAPI, 4',6-diamidino-2-phenylindole; RT-qPCR, reverse transcription quantitative polymerase chain reaction; TUNEL, terminal deoxynucleotidyl transferase dUTP nick end labeling.

SLC7A11 expression in CRC cells (*Figure 5A*). In addition, overexpression of *SLC7A11* significantly increased GSH levels in CRC cells, whereas MDA, ROS levels, and Fe^{2+} concentrations were significantly reduced (*Figure 5B-5E*). CRC cells overexpressing *SLC7A11* were injected subcutaneously into the lower abdomen of BALB/c nude mice. WB detection showed that compared with the sh-*circFADS2* + oe-NC group, the sh-*circFADS2* + oe-*SLC7A11* group showed an increase in *SLC7A11* expression in BALB/c nude mice (*Figure 5F*). After promoting *SLC7A11* expression, tumor growth and tumor weight significantly increased in BALB/c nude mice (*Figure 5G*). The results showed that overexpression of *SLC7A11* reversed the effect of knocking down *circFADS2* on promoting ferroptosis in CRC cells, indicating that *circFADS2* inhibits ferroptosis in CRC cells by regulating *SLC7A11* expression.

Discussion

CRC is the second deadliest cancer worldwide (23). Although improvements have been made in CRC treatment, the treatment and prognosis are still not ideal (24). Therefore, understanding the molecular mechanisms underlying the onset of CRC is crucial for improving the poor prognosis of CRC patients.

CircRNAs are involved in many different physiological processes, and many circRNAs are differentially expressed in CRC and matched normal tissues (25). *circFADS2* is the most significantly upregulated circRNA in CRC tissue (18). Therefore, we validated its role in CRC by knocking down *circFADS2*. We have demonstrated in our research that *circFADS2* plays an important role in CRC cells. After knocking down *circFADS2*, the cell proliferation and migration ability of CRC cells significantly decreased, whereas apoptosis significantly increased. This suggests that *circFADS2* may serve as a new breakthrough point for the treatment of CRC.

During ferroptosis, ROS production increases, mitochondrial volume decreases, and membrane density increases (26). It is often associated with lipid peroxidation caused by increased GSH consumption or lipid peroxidation, as well as *SLC7A11* deficiency (27). Ferroptosis has been shown to inhibit tumors (28). Our research results indicate that downregulating *circFADS2* significantly reduces the expression of *SLC7A11* in CRC cells. At the same time, the ROS and MDA levels in the cells were significantly reduced, the Fe^{2+} concentration was decreased, and the GSH level was increased. It was made clear that knocking down *circFADS2* promotes ferroptosis in CRC cells.

As a key regulatory protein of ferroptosis, *SLC7A11* has been reported to promote CRC progression (7). In addition, a study has shown that m6A methylation of *SLC7A11* mRNA plays a key role in the regulation of ferroptosis in CRC (29). *IGF2BP2*, as an m6A reader, can enhance mRNA stability by recognizing m6A modification sites (20). In oral squamous cell carcinoma, METTL3 enhances the stability of *SLC7A11* mRNA through m6A-mediated binding of *IGF2BP2* (21). To verify the mechanism by which *circFADS2* regulates *SLC7A11*, we demonstrated the interaction between *IGF2BP2* and *circFADS2*, as well as between *IGF2BP2* and *SLC7A11* mRNA, through RIP. It was demonstrated through nuclear cytoplasmic separation that *circFADS2* is mainly expressed in the cytoplasm. In addition, through stability testing of *SLC7A11* mRNA, we found that overexpression of *circFADS2* or increase of *IGF2BP2* can improve the stability of *SLC7A11* mRNA. We infer that *circFADS2* may regulate the stability of *SLC7A11* mRNA through *IGF2BP2*.

Afterwards, we demonstrated the co localization of *circFADS2*, *IGF2BP2*, and *SLC7A11* mRNA in the cytoplasm through IF-FISH analysis. Here, we provide an effective mechanism by which *circFADS2* enhances the stability of *SLC7A11* mRNA by promoting the formation of the *circFADS2/IGF2BP2/SLC7A11* mRNA protein complex. Although a previous study has shown that circFADS2 is the most significantly upregulated circular RNA in CRC tissues (18), no research has investigated the role and regulatory mechanism of *circFADS2* in CRC ferroptosis. Furthermore, we acknowledge that although we have demonstrated *in vitro* and *in vivo* that *circFADS2* inhibits ferroptosis in CRC cells by regulating *IGF2BP2*-mediated *SLC7A11* m6A modification, *in vitro* CRC cell lines and *in vivo* mouse models may not fully replicate all pathological features and immune responses of human CRC. This may affect the translatability of research results.

Our study demonstrates the molecular mechanism by which *circFADS2* inhibits ferroptosis in CRC cells by regulating *IGF2BP2*-mediated *SLC7A11* m6A modification. This offers fresh perspectives on the molecular process underlying CRC ferroptosis and lays a scientific foundation for developing new treatment strategies.

Conclusions

We have demonstrated that *circFADS2* can promote the

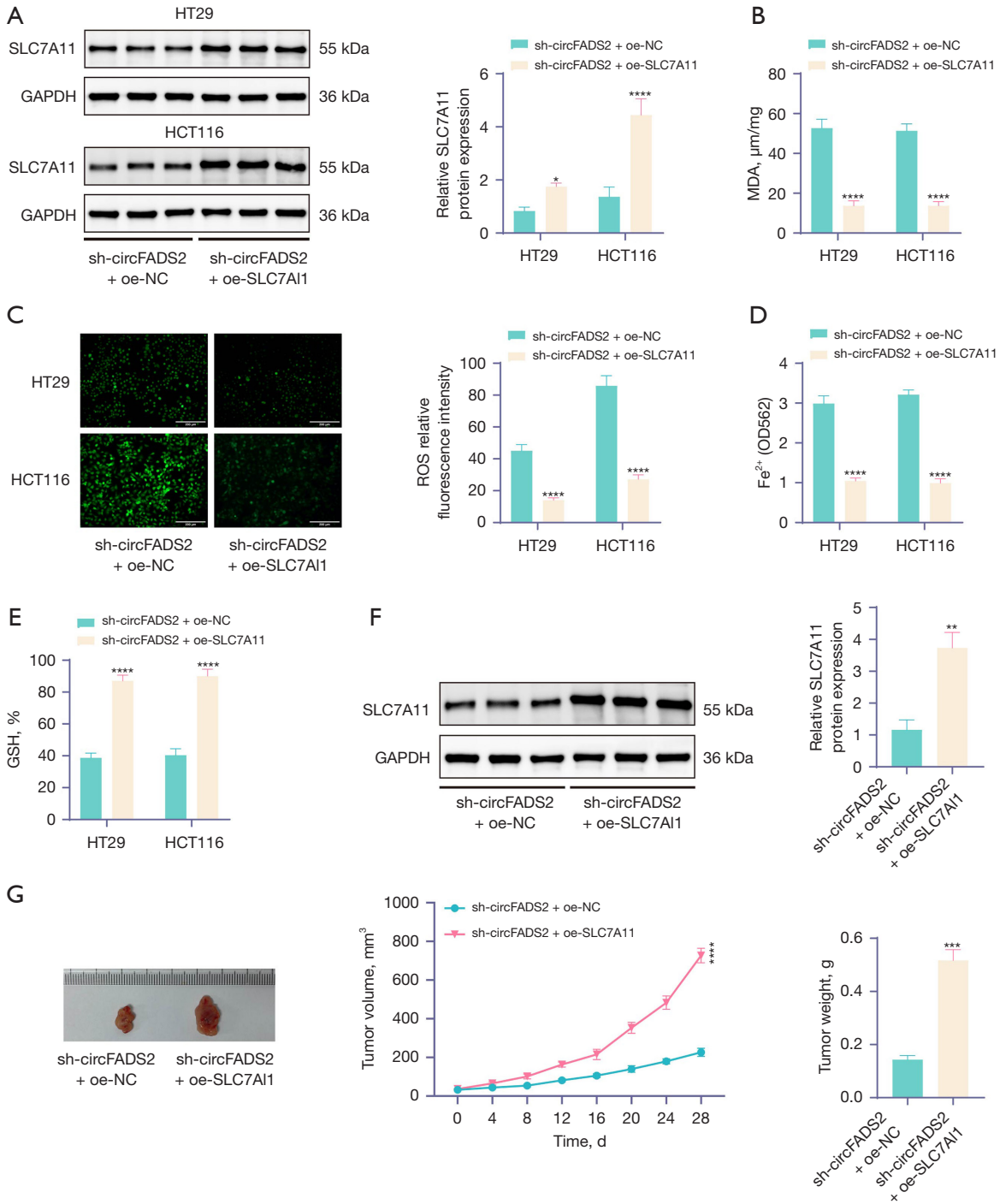

Figure 5 *circFADS2* inhibits ferroptosis in CRC cells by regulating *SLC7A11* expression. (A) WB detection of *SLC7A11* expression in CRC cells (n=3). (B-E) Detection of GSH, MDA, ROS, and Fe^{2+} levels in CRC cells (n=3). (F) WB detection of *SLC7A11* in mice (n=6). (G) Detect the volume and weight of xenografts in mice (n=6). Staining method: DCFH-DA staining (ROS assay). The magnification ratio of the image is 200 times (with a scale of 200 μm). *, P<0.05; **, P<0.01; ***, P<0.001; ****, P<0.0001. The detection between the two groups was analyzed using *t*-test. Two factor ANOVA will be used for three or more sets of data, and Tukey's will be used for post hoc testing. ANOVA, analysis of variance; CRC, colorectal cancer; DCFH-DA, 2',7'-dichlorodihydrofluorescein diacetate; GSH, glutathione; MDA, malondialdehyde; ROS, reactive oxygen species; WB, western blot.

formation of the *circFADS2/IGF2BP2/SLC7A11* mRNA protein complex, thereby promoting *SLC7A11* m6A methylation. This clearly promotes ferroptosis in CRC cells. This offers a fresh line of inquiry for CRC therapy and theoretical support for improving its poor prognosis.

Acknowledgments

None.

Footnote

Reporting Checklist: The authors have completed the ARRIVE and MDAR reporting checklists. Available at https://jgo.amegroups.com/article/view/10.21037/jgo-2024-1014/rc

Data Sharing Statement: Available at https://jgo.amegroups.com/article/view/10.21037/jgo-2024-1014/dss

Peer Review File: Available at https://jgo.amegroups.com/article/view/10.21037/jgo-2024-1014/prf

Funding: This study was supported by Natural Science Foundation of Hunan Province (Nos. 2024JJ7461; 2024JJ7465); Key Scientific Research Projects of Hunan Provincial Department of Education (No. 23A0348); Major Special Projects of Hunan Provincial Health and Family Planning Commission (No. A2017012).

Conflicts of Interest: All authors have completed the ICMJE uniform disclosure form (available at https://jgo.amegroups.com/article/view/10.21037/jgo-2024-1014/coif). The authors have no conflicts of interest to declare.

Ethical Statement: The authors are accountable for all aspects of the work in ensuring that questions related to the accuracy or integrity of any part of the work are appropriately investigated and resolved. This study was approved by the Animal Committee of Affiliated Nanhua Hospital, University of South China (No. 20240302) and conducted in compliance with the national guidelines for the care and use of animals.

References

1. Bhandari A, Woodhouse M, Gupta S. Colorectal cancer is a leading cause of cancer incidence and mortality among adults younger than 50 years in the USA: a SEER-based analysis with comparison to other young-onset cancers. J Investig Med 2017;65:311-5.
2. Liau XL, Salvamani S, Gunasekaran B, et al. CCAT 1- A Pivotal Oncogenic Long Non-Coding RNA in Colorectal Cancer. Br J Biomed Sci 2023;80:11103.
3. Ye S, Xu M, Zhu T, et al. Cytoglobin promotes sensitivity to ferroptosis by regulating p53-YAP1 axis in colon cancer cells. J Cell Mol Med 2021;25:3300-11.
4. Chen D, Chu B, Yang X, et al. iPLA2β-mediated lipid detoxification controls p53-driven ferroptosis independent of GPX4. Nat Commun 2021;12:3644.
5. Liu L, He J, Sun G, et al. The N6-methyladenosine modification enhances ferroptosis resistance through inhibiting SLC7A11 mRNA deadenylation in hepatoblastoma. Clin Transl Med 2022;12:e778.
6. Wang X, Chen Y, Wang X, et al. Stem Cell Factor SOX2 Confers Ferroptosis Resistance in Lung Cancer via Upregulation of SLC7A11. Cancer Res 2021;81:5217-29.
7. Shen L, Zhang J, Zheng Z, et al. PHGDH Inhibits Ferroptosis and Promotes Malignant Progression by Upregulating SLC7A11 in Bladder Cancer. Int J Biol Sci 2022;18:5459-74.
8. Yang J, Zhou Y, Xie S, et al. Metformin induces Ferroptosis by inhibiting UFMylation of SLC7A11 in breast cancer. J Exp Clin Cancer Res 2021;40:206.
9. Chen Q, Zheng W, Guan J, et al. SOCS2-enhanced ubiquitination of SLC7A11 promotes ferroptosis and radiosensitization in hepatocellular carcinoma. Cell Death Differ 2023;30:137-51.
10. Jiang L, Kon N, Li T, et al. Ferroptosis as a p53-mediated activity during tumour suppression. Nature 2015;520:57-62.
11. Qiao Y, Su M, Zhao H, et al. Targeting FTO induces colorectal cancer ferroptotic cell death by decreasing SLC7A11/GPX4 expression. J Exp Clin Cancer Res 2024;43:108.
12. Wang H, Breadner DA, Deng K, et al. CircRHOT1

restricts gastric cancer cell ferroptosis by epigenetically regulating GPX4. J Gastrointest Oncol 2023;14:1715-25.
13. Yao B, Zhang Q, Yang Z, et al. CircEZH2/miR-133b/IGF2BP2 aggravates colorectal cancer progression via enhancing the stability of m(6)A-modified CREB1 mRNA. Mol Cancer 2022;21:140.
14. Wang F, Nazarali AJ, Ji S. Circular RNAs as potential biomarkers for cancer diagnosis and therapy. Am J Cancer Res 2016;6:1167-76.
15. Xia H, Wu Y, Zhao J, et al. N6-Methyladenosine-modified circSAV1 triggers ferroptosis in COPD through recruiting YTHDF1 to facilitate the translation of IREB2. Cell Death Differ 2023;30:1293-304.
16. Chi F, Cao Y, Chen Y. Analysis and Validation of circRNA-miRNA Network in Regulating m(6)A RNA Methylation Modulators Reveals CircMAP2K4/miR-139-5p/YTHDF1 Axis Involving the Proliferation of Hepatocellular Carcinoma. Front Oncol 2021;11:560506.
17. Zhao F, Han Y, Liu Z, et al. circFADS2 regulates lung cancer cells proliferation and invasion via acting as a sponge of miR-498. Biosci Rep 2018;38:BSR20180570.
18. Xiao YS, Tong HZ, Yuan XH, et al. CircFADS2: A potential prognostic biomarker of colorectal cancer. Exp Biol Med (Maywood) 2020;245:1233-41.
19. Zhao BS, Roundtree IA, He C. Post-transcriptional gene regulation by mRNA modifications. Nat Rev Mol Cell Biol 2017;18:31-42.
20. Hou P, Meng S, Li M, et al. LINC00460/DHX9/IGF2BP2 complex promotes colorectal cancer proliferation and metastasis by mediating HMGA1 mRNA stability depending on m6A modification. J Exp Clin Cancer Res 2021;40:52.
21. Xu L, Li Q, Wang Y, et al. m(6)A methyltransferase METTL3 promotes oral squamous cell carcinoma progression through enhancement of IGF2BP2-mediated SLC7A11 mRNA stability. Am J Cancer Res 2021;11:5282-98.
22. Shen M, Cao S, Long X, et al. DNAJC12 causes breast cancer chemotherapy resistance by repressing doxorubicin-induced ferroptosis and apoptosis via activation of AKT. Redox Biol 2024;70:103035.
23. Long F, Li L, Xie C, et al. Intergenic CircRNA Circ_0007379 Inhibits Colorectal Cancer Progression by Modulating miR-320a Biogenesis in a KSRP-Dependent Manner. Int J Biol Sci 2023;19:3781-803.
24. Mi X, Yao H, Lu Y, et al. Leptin increases chemosensitivity by inhibiting CPT1B in colorectal cancer cells. J Gastrointest Oncol 2024;15:2507-20.
25. Zhou J, Wang L, Sun Q, et al. Hsa_circ_0001666 suppresses the progression of colorectal cancer through the miR-576-5p/PCDH10 axis. Clin Transl Med 2021;11:e565.
26. Jiang X, Stockwell BR, Conrad M. Ferroptosis: mechanisms, biology and role in disease. Nat Rev Mol Cell Biol 2021;22:266-82.
27. He F, Zhang P, Liu J, et al. ATF4 suppresses hepatocarcinogenesis by inducing SLC7A11 (xCT) to block stress-related ferroptosis. J Hepatol 2023;79:362-77.
28. Li D, Wang Y, Dong C, et al. CST1 inhibits ferroptosis and promotes gastric cancer metastasis by regulating GPX4 protein stability via OTUB1. Oncogene 2023;42:83-98.
29. Qiao Y, Su M, Zhao H, et al. Correction: Targeting FTO induces colorectal cancer ferroptotic cell death by decreasing SLC7A11/ GPX4 expression. J Exp Clin Cancer Res 2024;43:131.

Cite this article as: Jiang L, Lu X, Li W. *circFADS2* inhibits ferroptosis associated with *IGF2BP2*-dependent *SLC7A11* m6A modification in colorectal cancer cells. J Gastrointest Oncol 2025;16(2):503-516. doi: 10.21037/jgo-2024-1014

